

# Update on design simulations for NIF ignition targets, and the rollup of all specifications into an error budget

S.W. Haan<sup>a</sup>, M.C. Herrmann<sup>b</sup>, J.D. Salmonson, P.A. Amendt, D.A. Callahan, T.R. Dittrich, M.J. Edwards, O.S. Jones, M.M. Marinak, D.H. Munro, S.M. Pollaine, B.K. Spears, and L.J. Suter

Lawrence Livermore National Laboratory, P.O. Box 808, Livermore, CA 94551, USA

Received 15 February 2006 / Received in final form 15 June 2006

Published online 23 May 2007 – © EDP Sciences, Società Italiana di Fisica, Springer-Verlag 2007

**Abstract.** Targets intended to produce ignition on NIF are being simulated and the simulations are used to set specifications for target fabrication and other program elements. Recent design work has focused on designs that assume only 1.0 MJ of laser energy instead of the previous 1.6 MJ. To perform with less laser energy, the hohlraum has been redesigned to be more efficient than previously, and the capsules are slightly smaller. Three hohlraum designs are being examined: gas fill, SiO<sub>2</sub> foam fill, and SiO<sub>2</sub> lined. All have a cocktail wall, and shields mounted between the capsule and the laser entrance holes. Two capsule designs are being considered. One has a graded doped Be(Cu) ablator, and the other graded doped CH(Ge). Both can perform acceptably with recently demonstrated ice layer quality, and with recently demonstrated outer surface roughness. Complete tables of specifications are being prepared for both targets, to be completed this fiscal year. All the specifications are being rolled together into an error budget indicating adequate margin for ignition with the new designs. The dominant source of error is hohlraum asymmetry at intermediate modes 4–8, indicating the importance of experimental techniques to measure and control this asymmetry.

**PACS.** 52.57.-z Laser inertial confinement – 52.57.Bc Target design and fabrication – 52.57.Fg Implosion symmetry and hydrodynamic instability (Rayleigh-Taylor, Richtmyer-Meshkov, imprint, etc.)

## 1 Introduction

Targets have been designed for the campaign to attempt ignition on the National Ignition Facility [1] in 2010. These designs are very similar overall to those already discussed in detail in the literature [2,3]. The laser shines into circular holes in the ends of a high atomic-number cylinder, the interior of which heats up to a temperature of 300 eV with a carefully shaped prepulse. In the center of the cylinder is a spherical capsule, with an exterior shell of plastic or beryllium that ablates and implodes a layer of solid DT. Detailed descriptions are below. The purpose of the current work is to set requirements for the details of the target and associated fielding, primarily through the use of code simulations. The requirements are set so that the targets are projected to ignite, with some margin remaining, and so that they can be met with existing technology or plausible extensions thereof.

A representative design is shown in Figure 1. Key features of the designs being discussed here include:

- (i) use of a special material mixture (“cocktail”) for the hohlraum wall. The wall is currently projected to be

- (ii) shields between the capsule and the laser entrance holes. The shields improve the efficiency of the hohlraum and reduce the magnitude of the counterbalancing bright and dark views that determine P<sub>2</sub> asymmetry. How they affect the overall symmetry tune is still work in progress; optimization of modes higher than P<sub>2</sub> may be more difficult with the shields. Recent work on optimizing these hohlraums is described in reference [4];
- (iii) laser energy 1.0 MJ. The improvements described above in (i) and (ii), plus the use of beryllium for the ablator, or of layered dopants in CH, allow the use of less laser energy to drive the target, consistent with plans for facility start-up;
- (iv) micron-scale fill-tubes to fill the capsule with DT, rather than diffusion-fill. This reduces the cost and complexity of the cryogenic support system, since targets do not require cryogenic transport from a remote filling site;
- (v) three options for hohlraum fill: gas-fill, foam-fill, and lined. We are setting specifications for each of each of these. Figure 1 shows an SiO<sub>2</sub> foam filled hohlraum.

<sup>a</sup> e-mail: haan1@llnl.gov

<sup>b</sup> Now at Sandia National Laboratory, Albuquerque.

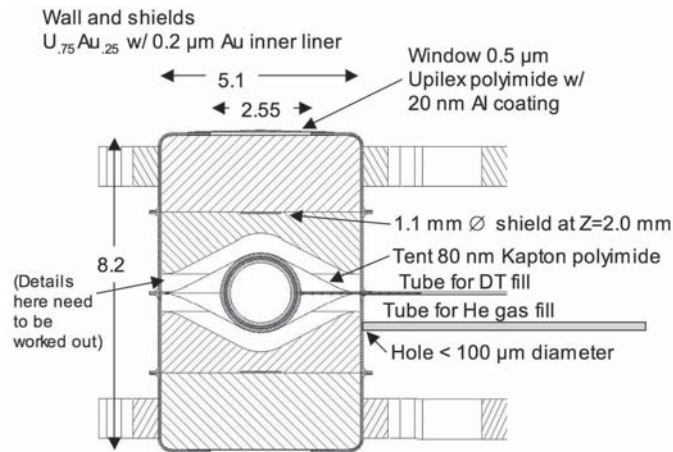


**Fig. 1.** Hohlraum, foam-filled. Detailed specifications are in spreadsheet, rendered drawings in (b) and (c). External details — flanges and support structure — are current engineering plans and are not part of the physics specifications. The foam stands off from the capsule by  $500\ \mu\text{m}$ , and a gap is allowed at the waist that is to be less than TBD  $\mu\text{m}$ .

In the current design the capsule is only 10% smaller in radius than capsules that were designed to be driven with 1.6 MJ, instead of being 15% smaller as would be projected by energy scaling. The use of beryllium for this slightly smaller capsule makes it virtually equivalent to the 1.6 MJ designs using plastic ablators at 10% larger radius.

We are setting specifications for a number of configurations of the target. There are three ablator options: beryllium with layers of Cu dopant, beryllium with uniform Cu dopant, and CH plastic with layers of Ge dopant. The uniform-Be design is being specified by Los Alamos and is not discussed in this article. All of the capsules assume  $0.3\ \text{mg/cc}$  central DT gas density, and the use of higher density appears to be precluded by the assumption of 1.0 MJ. Any of these could be fielded in any of three hohlraum options: He gas filled,  $\text{SiO}_2$  foam filled, or lined with  $\text{SiO}_2$ .

Detailed specifications are being set for all three hohlraum options, and all three capsule options. They are summarized herein. Fully detailed specifications will be established and publicly “frozen” as of 1 Oct. 2005. Subsequent changes will be subject to review and agreement by a change control board. At any time after 1 Oct. 2005 the current specifications will be available from the first author at the e-mail address given above.

The remainder of this document is: Section 2: Target configuration and options; Section 3: Procedure for setting and rolling together the specifications; Section 4: Rollup into a net error budget; Section 5: Summary discussion.

## 2 Target configuration and options

The generic hohlraum/capsule configuration is shown in Figure 1. The innermost hohlraum surface is Au,  $0.2\ \mu\text{m}$

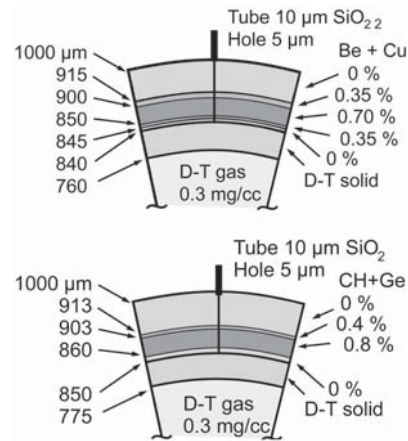


**Fig. 2.** The two capsule designs discussed herein. Both designs use graded dopants, have the same outer radius, and are driven at 300 eV with essentially identical requirements for laser power and energy.

thick. This is backed with at least  $7\ \mu\text{m}$  of a “cocktail” mixture of U and Au, and at least  $3\ \mu\text{m}$  of additional Au. Anything outside the  $10\ \mu\text{m}$  layer does not affect the performance of the hohlraum, except along several lines of sight: star-pattern windows along two perpendicular directions, for cryo layer characterization; a window for X-ray imaging of the core; and a clear area for neutron imaging of the core. All of these lines of sight are at or near the waist plane, with allowances that are being specified. The lip of the laser entrance hole (LEH) is coated, either with CH or, in the case of the  $\text{SiO}_2$  lined hohlraum, with  $\text{SiO}_2$ . The hohlraum has LEH shields, which at this time are to be made of the same cocktail material as the hohlraum wall including the gold coating. It may be acceptable to fabricate these from Au rather than cocktail, and this is one of the issues listed as a possible future change, to be investigated further. The LEH shields are coated with CH, except on the side facing the capsule. The shields are supported with polyimide sheets with holes as needed for gas flow. The capsule is supported with a polyimide tent. Figure 1 shows other external details (the flanges, and support system) which are not part of the physics specifications but are part of the current engineering plan.

The interior of the hohlraum is different in the three hohlraum options. The design shown in Figure 1 is filled with  $\text{SiO}_2$  foam at density  $10^{-3}\ \text{g/cc}$  and He gas for thermal conduction, at  $10^{-5}\ \text{g/cc}$ . The gas-filled hohlraum option is filled with He gas at  $1.3 \times 10^{-3}\ \text{g/cc}$ . The lined hohlraum is coated on the inside with  $\text{SiO}_2$ ,  $0.5\ \mu\text{m}$  thick. It is also filled with He for thermal conduction, at  $10^{-5}\ \text{g/cc}$ . The lined hohlraum requires a generically different laser pulse, with a small prepulse to blow down the liner before the full foot power is delivered. The lined and foam-filled hohlraums have thinner windows over the LEH.

Two ablator options are described in this article: graded doped Be(Cu), and graded doped CH(Ge). The two designs are shown in Figure 2. The Be(Cu) design is a scale of the design described in reference [5]. The most important difference between the CH and Be designs is the larger ablator mass in the layered beryllium target. All targets have very little ablator remaining at peak velocity; having more mass ablated makes for better ablation

stabilization, improving the stability features for the mid-range modes (10–100) for which ablation stabilization is important. At lower modes there is little stabilization and the targets are essentially equivalent; at higher modes, the most important stability feature is coupling to, and growth at, the ablator-DT interface, which are determined by the preheat characteristics of the ablator. A uniformly doped Be design is also being planned, with details being developed by Wilson et al. at Los Alamos National Laboratory [6]. At this time any of these three capsules could be considered as driven by any of the three hohlraum options.

### 3 Procedure for setting and rolling together the specifications

Specifications are set using simulations of the growth and/or impact of the various deviations between the ideal implosion and plausible expected reality. Four kinds of simulations are being used. All the implosion-only simulations use an opacity model [7] that combines STA [8] for the Cu and OPAL model for the Be [9]. The 2D implosion-only simulations use a few-group opacity scheme developed by one of us (M. Marinak) that is equivalent to using highly-resolved STA/OPAL opacities. All simulations used equation of state QEOS [10] with parameters set for DT so that the first shock Hugoniot represents a reasonable consensus of recent experimental activity [11].

#### 3.1 Integrated hohlraum/capsule simulations

These are 2D or 3D simulations of the entire target with full radiation transport. All the target physics is included except microscopic laser-plasma interactions, and hydrodynamic instability in modes above about 8. These simulations use non-LTE XSN [12] for the opacities and ionization state, and use QEOS equation of state. They serve several purposes: determine the laser pulse needed to drive the target; ensure that the liner/fill combination keeps the hohlraum open, with acceptable spurious pressure on the capsule (“hydro-coupling”); indicate an optimum pulse shape, symmetry, and energetics configuration for the hohlraum; and provide drive spectra for the capsule-only simulations described below. An integrated simulation with optimal symmetry and pulse-shaping provides the central point for sensitivity studies in which the laser or target geometry is varied. Such studies have been done in the past for a number of targets and are in progress for the new 1.0 MJ targets. More details on recent results for the current designs are in reference [3].

#### 3.2 One dimensional capsule-only simulations

In one dimension (1D) capsule implosions we consider variations in capsule dimensions, densities, dopant concentrations, pulse shape, and drive spectrum. These are considered one at a time, and in random combinations assuming Gaussian statistics with specified root mean square

deviations. Results are described in the following section. We will call the 1D deviations from nominal “perturbations” although in ICF this term is more commonly used for 2D or 3D perturbations.

#### 3.3 Growth factors and linear analysis

In two dimensions (2D), simulations of the capsule implosion are done with infinitesimal perturbations to determine “growth factors”, that is, the ratio of the final perturbation amplitude to the initial perturbation. Initial amplitudes are chosen to be large enough to dominate numerical noise, but small enough that perturbations remain proportional to the initial amplitude. Perturbations are imposed in the form of single Legendre polynomial modes; the growth factor for any 3D spherical harmonic perturbation is thereby known. Growth factor curves vs. mode number are determined for initial perturbations on each of the seven interfaces, and for density variations. The density variations are used to set specifications for voids in the beryllium and DT. For these we must assume a radial dependence; so far we have considered density perturbations independent of radius in the ice, independent of radius in the beryllium shell overall, and in the first layer of the beryllium. The perturbations seeded by density variations grow to be similar to those seeded by surface perturbations at the nearest unstable surface, when initialized with the same initial column density variation.

The growth of short wavelength perturbations depends on the spectrum of the X-rays driving the implosion. X-ray preheat during the acceleration phase of the implosion changes the density profile somewhat, but the density profile during acceleration does not vary enough to cause significant difference in the growth *rate*. However, early time preheat in the SiO<sub>2</sub> filled hohlraum significantly affects the early time evolution of high mode perturbations on the inner surface of the ablator for the layered targets — the doped part of the shell expands after preheat and crushes the innermost undoped layer and nearby fuel. This reduces the initial amplitude of high mode perturbations — modes 200–500, with wavelengths 5–30  $\mu\text{m}$ , that are short enough to be affected by this  $\mu\text{m}$ -scale motion. If we were confident of the physics of this effect, and confident that we would only field SiO<sub>2</sub> filled hohlraums, we could loosen the specification for high modes on this surface. However, since the other hohlraums do not produce this reduction, and because it is a new physics phenomenon that needs to be understood better, the specifications correspond to the situation with the most growth: they use the spectrum in the gas-filled hohlraum, with the cocktail wall.

For sufficiently small perturbations, the perturbation at any time of interest can be obtained by simulation-based linear analysis, which combines “growth factors” with an assumed initial spectrum of perturbations. Single-mode simulations are used to obtain growth factors, which are the ratio of the perturbation at the time and interface of interest to the initial perturbation. Representative growth factor curves are shown in Figure 3. Considerable

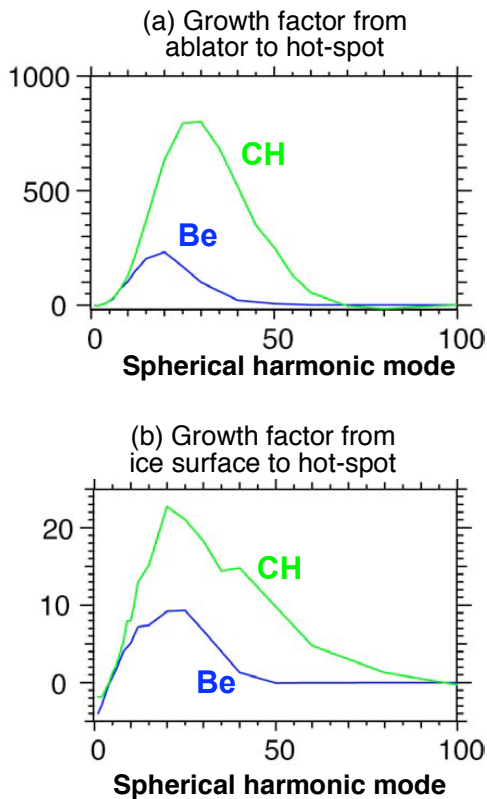


**Fig. 3.** Growth of single-mode surface roughness perturbations seeded by ablator roughness (a) and ice roughness (b), for the two graded-doped designs. Final perturbations are evaluated as deformations of the hot-spot perimeter when the central ion temperature is 12 keV. Because the CH has more growth of ablator roughness perturbations, the specifications for the outer surface roughness are tighter for CH than for Be. For the ice perturbations, this is probably not possible and the larger growth reduces the margin of the CH design.

effort has gone into designing the targets to minimize the growth.

The growth factors are combined in linear analysis with assumed spectra of initial perturbations, to determine final perturbations. Representative initial spectra are shown in Figure 4. The linear analysis combining growth factors and initial spectra is fully 3D, and is as accurate as the linear-regime 2D simulations if the perturbations are small enough to remain linear. It is less accurate for the density variations, since they can only be simulated for an assumed radial variation which does not correspond to voids in the same “exact” way that surface perturbations are described in the simulations. Final perturbations are considered at two times: peak velocity and ignition time. The perturbations on the hot-spot at ignition are predominantly in modes below about 20; which source of perturbation dominates will be described below when the rollup is discussed. At peak velocity the dominant perturbations are at much shorter wavelength (modes 100–400). Their impact is discussed below.

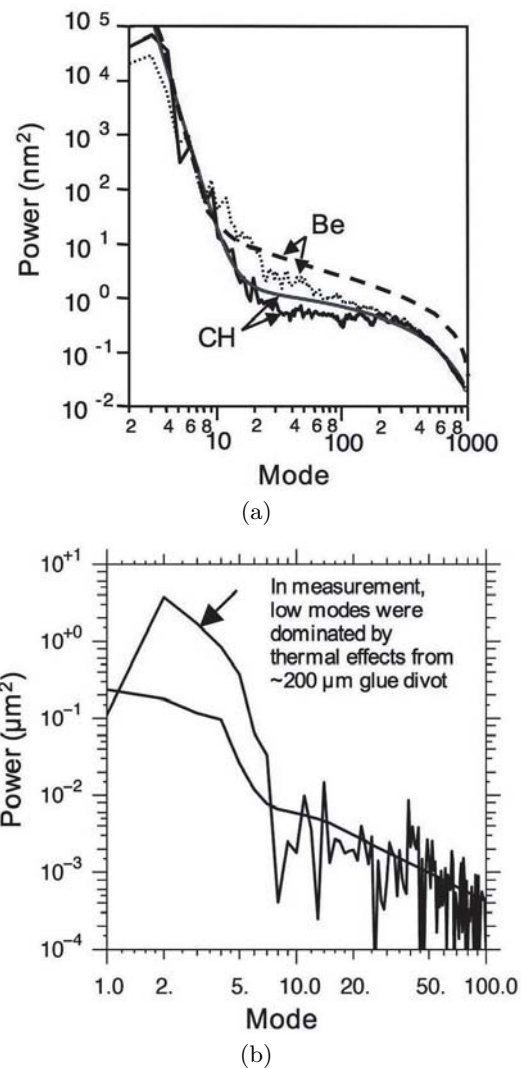


**Fig. 4.** Power spectra of initial surface roughness. Smooth curves are requirements for the outer surface (a) and ice (b) of the Be and CH designs. Rough curves are target fabrication data. These are power spectra of great-circle traces on the surfaces.

### 3.4 Large amplitude 2D and 3D capsule-only simulations

Linear analysis gives us an estimate of how large the perturbations are expected to be, but does not tell us how large they are allowed to be or whether nonlinear effects are important. For that we use simulations with larger-than-specified initial perturbations, in order to find the “cliff” in performance. In the past, for other designs, these simulations have been done in 3D, and 3D simulations are in progress for the new designs but are not ready to be described here. The character of the final perturbations, in 2D or 3D, is only very weakly dependent on how the perturbations were seeded, since the growing perturbations settle into an eigenmode, and “find” the dominant modes regardless of seed. The main parameters determining the performance are the overall amplitude of

the perturbations, and the dominant mode, regardless of seed. Various combinations of initial seeds result in the same final characteristics, and their relative contributions are accurately described (relative to the simulations) by linear analysis.

Multi-mode simulations with larger-than-specified initial perturbations, with realistic power spectrum, indicate that growth to peak velocity is very close to linear up to modes above 500, for initial perturbations around those specified. The perturbations on the outside at peak velocity are large compared to the wavelength, but the growth is largely due to a “taffy pull” expansion that does not go into nonlinear saturation in the way that Rayleigh-Taylor perturbations are known to in circumstances with different interplay of compressibility and convergence. These perturbations grow on the interface between the fuel and the beryllium, at the late stages of the acceleration when that interface is unstable. Their growth varies substantially from one target design to another. At very high modes (above 1000) the growth is expected to be reduced by diffusion and viscosity [13]. This is also described accurately by linear analysis, if the code uses a good model for diffusion and viscosity. Validating our current modeling in this regime is an area of active design work. We have done 2D multi-mode simulations with angular zoning adequate to resolve modes up to about 1000 as seeded by the nominal perturbation on the DT/Be interface, showing a result very close to that expected from linear analysis. At moderately high modes — 500 to 1000 — it is not clear how important nonlinear effects might be. For these modes, on the outside at peak velocity, the saturation model from reference [14] is used. This affects primarily the perturbations seeded by voids, and better 3D modeling of these is an area of active investigation.

On the inside at ignition time, the as-specified perturbations are very close to being linear. Between the as-specified perturbations and the “50% yield” perturbations, nonlinear saturation begins to be important. Hence the multiplier needed on the initial perturbations to cause failure is considerably larger than the “margin” quoted below, which is the multiplier needed on the final perturbation to cause failure.

With large-amplitude simulations we see the two failure modes mentioned above. At peak velocity the perturbations result in beryllium “bubbles” penetrating the fuel from the outside. The fuel in the “spikes” surrounded by these bubbles does not burn, later on after ignition. Thus this penetration must be kept small enough to allow an acceptable yield. This is not necessarily hard failure, and in principle it could end up that we accept considerable mix penetration and yield reduction. Dominant modes are 100–400. Currently specifications are set so that the yield reduction is less than about 10%. The other failure mode is at ignition time, when spikes of cold high-density DT penetrate the hot spot and cool it as it is trying to ignite. This is hard failure as it can prevent ignition. Dominant modes are 5–25. The lower modes dominate not because of non-linear saturation, but because the high modes do not couple through the shell to grow on the inside around igni-

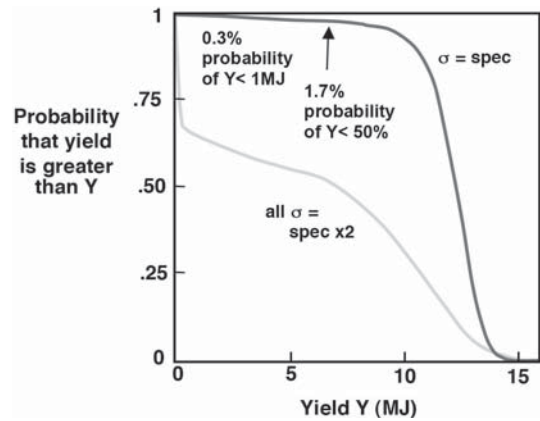


**Fig. 5.** Result of a large number of 1D simulations with randomly chosen errors. For the upper curve, the errors were chosen from a set of normal distributions with each standard deviation equal to the specification. A large majority of these simulations burned to yield above 10 MJ, and 98.3% gave yield above 50% of the nominal yield. For the lower curve, the standard deviation for all of the errors was twice the specification. With these wider distributions, 50% of the simulations gave yields above 50% of nominal, so we say that in 1D the net rollup is 50% of the distance to the cliff.

tion time. This is evident in Figure 3 where the high modes do not show very much growth. This failure mode can be enhanced by 1D errors, since 1D errors reduce margin, delay ignition, and increase the deceleration Rayleigh-Taylor growth. In simulations that combine a 1D error with a hot-spot 2D error, we find that their impact is close to being described via a quadrature sum of the two effects. This is shown in more detail below. In the specifications as described below, the 1D and 3D errors are almost equally balanced, with net impact being about  $\sqrt{2}$  times each individual contributor.

Growth of high modes on the outside during acceleration is coupled to 1D errors in a more complicated way. Recall that the impact of the high modes is to cause mix, keeping the outer part of the fuel from burning. Small 1D errors that reduce margin, while they increase deceleration growth and are thereby coupled to hot-spot perturbations, do not affect high mode growth. Thus it is probably not appropriate to combine the high mode degradation in quadrature with the 1D errors (or with the low mode growth). However, 1D errors that change the density profiles or ablation rate during acceleration can change the growth factors themselves. How to incorporate this in the rollup modeling is still being considered.

#### 4 Rollup into net error budget

As well as possible, all of the sources of uncertainty are combined into a net rollup. The various 1D sources of uncertainty are all small enough that by themselves they do not significantly affect the performance, although they do in combination. Table 1 shows the individual 1D errors, their specifications, and their contributions. Figure 5

**Table 1.** 1D sources of error. For each source of error or uncertainty we show the part of the program responsible for achieving this requirement, the required value, and the highest multiple of the nominal requirement that returns at least 50% yield, in simulations in which that is the only error. Multipliers beyond 8 were not considered, and a table entry “>8” indicates that the yield is >50% with a multiplier of 8. The net rollup is based on statistical combinations as shown in Figure 5. The fourth shock is clearly the dominant source of uncertainty in 1D.

For each of 27 parameters we have a requirement $\sigma$ , and have identified how large a variation can be tolerated in that parameter if varied singly. Sensitivities in 1D only:			
Parameter	Responsibility	Requirement $\sigma$	(50% yield pt) / $\sigma$
<b>Capsule dimensions</b>			
Outer radius	Fab	3 $\mu\text{m}$	> 8
Be thickness, average density (shot to shot)	Fab	2 $\mu\text{m}$ , 1%	> 8, > 8
Solid DT thickness	Cryo	1.0 $\mu\text{m}$	> 8
Radial of 4 dopant steps	Fab	0.5, 1, 2, 2 $\mu\text{m}$	all > 8
Dopant concentrations (3)	Fab	15, 10, 15%	8, 6, > 8
Oxygen in Be	Fab	0.4%	6
Argon in Be	Fab	0.08%	8
H in DT	Cryo	0.05%	> 8
<sup>3</sup> He in DT	Cryo	24 $\pm$ 12hrs	8
DT gas density (temperature)	Cryo	10%	> 8
<b>Pulse-shape parameters</b>			
Initiation (foam density, window thickness, etc.)	Fab	100ps	6
Time of 2nd, 3rd shocks	Shock timing	50 ps	>8, 8
Time of 4th shock	Shock timing	100ps	3.2
Time of peak pulse, relative to 4th shock	Shock timing	100ps	8
Level of shocks (uncertainty from wbs3, laser)	Shock timing	% flux: 3,3,3,5	6, 8, 8, 6
Multiplier on M-band part of spectrum	Shock timing	30%	> 8
Reproducibility of laser pulse (time dependent)	Shock timing	3% to 1.5%	> 8
<b>Net rollup (either quadrature sum, or overall variations)</b>			<b>1.9</b>

shows a statistical summary of a large number of runs with various combinations of 1D errors. See the caption of Figure 5 for a discussion of the result. (Note: Fig. 5 was generated with XSN opacities and shows slightly more robust performance than what is seen with the more detailed STA/OPAL opacities. This work is currently being updated.) The overall margin of 2 is dominated by the 4th shock sensitivity, but that sensitivity alone is by no means responsible for the entire rollup. Its relative impact can be estimated from Table 1, and from the estimate that we have a factor of two overall margin: in the overall quadrature sum of all 1D errors, which adds to  $0.25 = 1/2^2$ , the part due to the 4th shock timing is  $1/3.2^2 = 0.1$ . So the largest single error is very important but is far from being solely responsible for failures.

In 3D the errors are rolled up together by using growth factors and assumed initial power spectra. This gives an estimated “final” perturbation, but does not tell us how large of a perturbation is allowed. As described above, the allowable perturbation is determined by simulations with large initial perturbations. Figure 6 shows how large the surface roughness perturbation can be, and Figure 7 the P6 asymmetry. Future work is needed to address wider spectra of modes, and combinations of sources of uncertainty.

For voids in the beryllium or the DT, there are two separate issues. First, the average density affects the 1D hydro — the key issue is reproducibility of the density from shot to shot. This is specified as “average density” and is

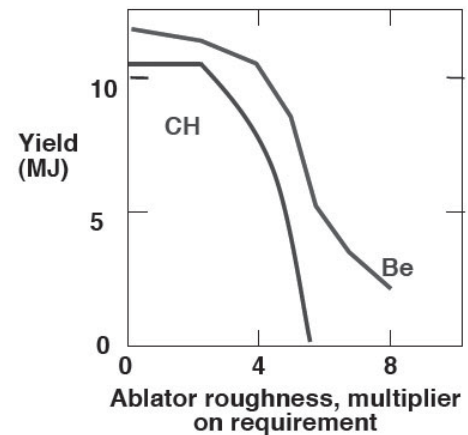


**Fig. 6.** Yield vs. ablator roughness, shown as a multiplier on the specified roughness. These simulations included modes 12–160 and are dominated by mode 12 at ignition time.

specified as 2% absolute and 1% shot-to-shot-variability for the ablaters, and twice that for the DT. The other more complex issue pertinent to voids is lateral variations as a seed for Rayleigh-Taylor instability. Current specifications on the lateral density variations assume that the voids are randomly located, that they have a characteristic volume, and that the total void density is known. This then determines the number of voids, and simple statistics describes the variations in column density. For the beryllium we specify that the void fraction, as it determines

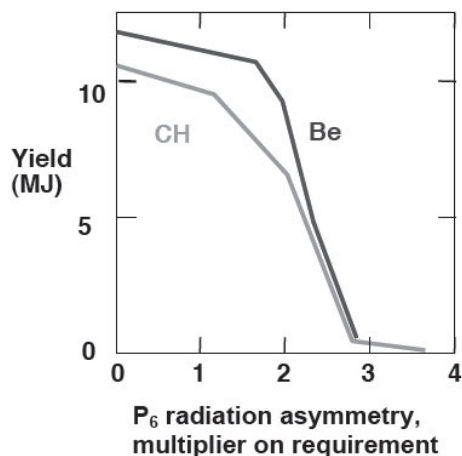


**Fig. 7.** Yield vs.  $P_6$  asymmetry, constant in time. In this case the acceptable multiplier is smaller than in Figure 6, indicating that there is less margin above the specification.

lateral variations, is less than 2%, and that the characteristic void volume is less than  $0.15 \mu\text{m}^3$ . Actually only the product, (void density)  $\times$  (void volume) determines the column density variations. We expect the voids to be characterized by radiographic transmission, and if our assumptions about random location etc. are not valid, then to first order their impact on the implosion is still adequately characterized: the impact on the implosion, and the signature in radiographic characterization are both determined by the column density. So the specification is “the voids need have the same impact on lateral variations in integrated column density as if they were randomly located with volume  $0.15 \mu\text{m}^3$  and void fraction 2%”. We have estimated the variations in optical depth that arise in radiographic characterization of the shells, and the current plan of measuring to  $1:10^4$  should be adequate to see the lateral column density variations resulting from the currently specified voids. To a very rough first approximation the same is true for opacity variations, although in this case the relative impact is somewhat different. In the case of opacity variations, it appears that radiographic characterization is actually more sensitive than necessary, so that transverse variations in oxygen, argon, and/or copper will be constrained not by implosion requirements directly, but by the requirement that they be small enough to allow characterization of the void structure in the beryllium. For the layered targets, with the specified internal layer roughnesses, the modulations in transmission caused by internal layer roughness may again be too large for us to effectively see the modulations caused by voids or other internal structure. (A quantitative analysis of this is possible, and is in progress.) If that is the case, that is, if the internal surfaces turn out to be too rough to allow void characterization but smooth enough to meet the implosion requirements, then radiographic characterization can be done with capsules that are not actual ignition capsules (e.g. an entire shell of undoped or uniformly doped beryllium), to ensure that the process creating the material results in acceptable lateral variations caused by the

void structure. In any case, radiographic characterization on fully layered capsules will be valuable to ensure the quality of the internal layers as well.

The beryllium design could be subject to perturbations seeded by the movement of the first shock across the grain structure in the ablator. If the material is melted before or at passage of the first shock, it is less likely that such perturbations will be seeded. The design for which most of the results are presented here — driven with a gas-filled cocktail hohlraum — has the first shock intentionally strengthened so that it is strong enough to melt the beryllium.

The ice roughness requirement is shown in Figure 4, along with the measured ice roughness [15]. In this case there is no reason to expect that the ice can be smoother in CH than in Be and the two targets have the same specification. The ice perturbations have a relatively larger impact in the CH target. The noisy curve in this case is the demonstrated ice roughness. At low modes the spec is tighter than has been demonstrated, but the experiments so far have been dominated by a large fill tube that affects the thermal distribution.

Simulations have been done of various configurations of fill tubes and holes. The currently assumed configuration of a 10-micron glass tube, over a 5-micron hole in the ablator, appears to be acceptable for both ablator materials. Simulations of the perturbations seeded by these tubes are described in reference [16].

The procedure just described has been applied to the Be(graded Cu) and CH(graded Ge) targets shown above. The growth factors for perturbations initially on the outside of the ablator, and on the ice, are shown in Figure 3. Specifications that result in acceptable performance are similar to what has been demonstrated for these materials. The Be target is allowed to be somewhat rougher than CH, because the implosion is more stable. The noisy curves overplotted are characterization results for the two materials (the beryllium has been polished). Except for a possible issue with Be at modes around 15, the demonstrated surfaces meet the specifications.

Figures 8 and 9 show the rollup of the 3D errors on the hot-spot boundary, and Figure 10 the rollup of perturbations on the outside of the shell at the time of peak velocity. At peak velocity (Fig. 10) the maximum acceptable perturbation is  $15 \mu\text{m}$ ; for this final perturbation, the yield will be degraded by about a factor of two by mix of beryllium with the outer part of the fuel. For the hot-spot (Figs. 8 and 9) the 50% yield “cliff” depends on what modes dominate, as indicated by the yellow curves in Figures 8 and 9. These are based on simulations such as those shown in Figures 6 and 7.

In both 1D and 3D, considered separately, the layered Be target has about 100% safety margin in the size of the perturbations — that is, if all the parameters were away from nominal by twice the specification, we would expect with 50% probability a yield of 5–7 MJ. Most combinations of errors that are equivalent to this overall factor of two, in a quadrature sum sense, would have similar impact. There remains the question of how 1D and 3D errors



**Table 2.** Comparison of key parameters for layered Be and layered CH capsules. Quantities not in bold are results of simulations for the indicated issues. Quantities in bold are estimates of margin based on inverse-quadrature summation of the full spherical harmonic spectrum for both the issues indicated and other issues, which are equivalent for Be and CH. Margin in 1d is reduced slightly in CH since sensitivity to 4th shock is tighter. Ablator margin is the same since the ablator specs are tighter for CH. Ice is assumed to be the same initial roughness, and has more impact on the less stable CH capsule. This reduces the 3D margin somewhat, so that the net margin is reduced from 1.34 for Be to 1.22 for CH.

	<i>Be(Cu)</i>	<i>CH(Ge)</i>	<i>Remark</i>
Eabs (kJ)	139.00	107.00	
Yield (MJ)	13.00	10.40	
Fuel Mass (mg)	0.161	0.156	
Ablator Mass (mg)	3.190	1.760	
Peak $\rho r$ (g/cm <sup>2</sup> )	1.920	1.700	
Implosion Velocity (10 <sup>7</sup> cm/s)	3.70	3.86	
FWHM of Yield Versus 4th Shock Timing	640 ps	510 ps	
Net 1D margin	1.90	1.79	CH slightly tighter, 4 <sup>th</sup> shock
Atwood Number at Interface	0.25	0.25	
Cliff for High Mode Surface Roughness (nm)	300.00	90.00	
Cliff for Intermediate Mode Ablator Roughness (6-36)(x NIF Standard)	4.00	3.00	
Ablator margin	5	5	Spec set so margin same
Cliff for Constant In-Time Negative P6 Asymmetry	0.50%	0.50%	
Asymmetry margin	2.	2.	Low mode sensitivity same
Cliff for Intermediate Mode Ice Roughness (6-36) X Measured Roughness at -1.5K	3.0-4.0	1.5-2.5	
Ice margin	4	2.5	Ice roughness same, more growth for CH
Net 3D margin	1.90	1.67	Asymmetry most important,
Net margin 3D & 1D	1.34	1.22	

1D and 3D margin is not appropriate, because changing the central gas composition actually increases the 1D yield — converting DT to <sup>3</sup>He at fixed total density increases the yield by delaying ignition so that the target burns at higher  $\rho R$ . But that delay increases deceleration-phase Rayleigh-Taylor growth so that the target is more susceptible to roughness perturbations. Figure 12 shows the combined impact of <sup>3</sup>He, indicated as DT age, with surface roughness. The current specification seems justified.

For the plastic capsule, the overall margin is somewhat smaller. A comparison of the Be and CH capsules is in Table 2. The most significant difference is in the high-mode surface roughness, which is a factor of about 3 different. This is reflected in different specifications for the ablator roughness. At lower modes the CH target is about as sensitive as the Be capsule, which is important because those are the modes that dominate the margin in 3D. The ice sensitivity is determined by intermediate modes and

for CH it would be appropriate to spec the ice tighter by ~50%. However it is unlikely that this can be met and the specification has been left the same, so the margin is reduced. Similarly, the shock timing requirement should be tighter by 5/7, but since it seems unlikely that this could be met, it results in less margin for the CH target. The net impact of the differences, as shown in Table 2, is that the CH target has margin 1.22 while the Be target has margin 1.34.

## 5 Concluding remarks

One inference to be drawn from this work is the ranking in significance of the various sources of error. The specifications fall into three categories, each of which is responsible for about 1/3 of the rollup: (i) the dominant uncertainties of hohlraum asymmetry in 3D and 4th shock in 1D;

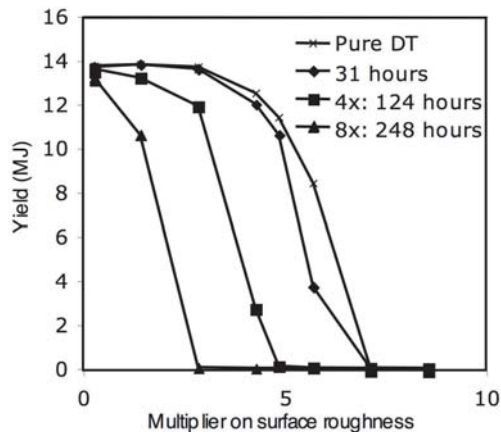


**Fig. 12.** Yield vs. surface roughness for various amounts of  $^3\text{He}$  added to the central DT gas. The amount added assumes that the DT had aged for the indicated amount of time, and that all of the  $^3\text{He}$  from all of the fuel is in the gas. As the DT ages, the performance becomes more sensitive to growth of Rayleigh-Taylor perturbations during the deceleration phase, and the surface roughness specifications would have to be tighter.

(ii) a handful of items which are significant contributors but not nearly as large as items (i); and (iii) a large number of small items. Category (i) issues are the responsibilities of the symmetry and shock timing programs and we must do what we can to bring them down. They cannot be improved by simply asking for a tighter spec. Category (ii) issues are those with 8 or less in the right column of Table 1, and all of the curves other than asymmetry in Figures 8 and 9. These are mostly target fabrication: surface roughnesses, the details of the layers, target dimensions, etc. These could in principle be traded off against each other, but if any of them are loosened others should be tightened. Tightening any one of them has little impact, but tightening them all would increase the margin somewhat. Category (iii) issues are those  $>8$  in Table 1, and most of the hohlraum details that are set to be good enough that they have negligible impact. (Note that the hohlraum foam density, for the foam-filled hohlraum, is in category (ii) as it affects the foot of the pulse.) These are currently thought to be relatively straightforward to achieve and are important only in that there are many of them. Those specifications could be loosened if necessary but of course caution is required.

The other important conclusion that we draw is that ignition at 1.0 MJ looks viable, with reasonable specifications for the target and programs. There is enough margin

(1.34 and 1.22 for the two targets) to leave some room for error, but not enough for very large errors, especially in the dominant contributors. It is important that all specifications be met (except possibly some of those in category (iii) above), and if they are met we have good reason to expect ignition in 2010.

Work performed under the auspices of the US Department of Energy by the University of California, Lawrence Livermore National Laboratory under Contract No. W-7405-ENG-48.

## References

1. J.A. Paisner, J.D. Boyes, S.A. Kumpan, W.H. Lowdermilk, M.S. Sorem, *Laser Focus World* **30**, 75 (1994)
2. J.D. Lindl, *Inertial Confinement Fusion* (Springer-Verlag, New York, 1998)
3. S.W. Haan et al., *Phys. Plasmas* **2**, 2480 (1995)
4. D.A. Callahan et al., *Phys. Plasmas* **13**, 056307 (2006)
5. S.W. Haan, M.C. Herrmann, T.R. Dittrich, A.J. Fetterman, M.M. Marinak, D.H. Munro, S.M. Pollaine, J.D. Salmonson, G.L. Strobel, L.J. Suter, *Phys. Plasmas* **12**, 056316 (2005)
6. D. Wilson, private communication
7. J. Castor, private communication
8. A. Bar-Shalom, J. Oreg, *Phys. Rev. E* **54**, 1850 (1996)
9. F.J. Rogers, C.A. Iglesias, *Science* **263**, 50 (1994); C.A. Iglesias, F.J. Rogers, *Astrophys. J.* **464**, 943 (1996)
10. R.M. More, K.H. Warren, D.A. Young, G.B. Zimmerman, *Phys. Fluids* **31**, 3059 (1988); for specifics of the Hugoniot used here see A. Fetterman et al., *Phys. Plasmas* (submitted 2006)
11. T.R. Boehly et al., *Phys. Plasmas* **11**, L49 (2004); M.D. Knudson et al., *Phys. Rev. Lett.* **90**, 035505 (2003); G.W. Collins et al., *Phys. Plasmas* **5**, 1864 (1998)
12. See National Technical Information Service Document No. UCRL-52276 [W.A. Lokke, W.H. Grasberger, in Lawrence Livermore National Laboratory, UCRL-52276, (1977)]; copies may be ordered from the National Technical Information Service, Springfield, Virginia 22161, the price is \$19.50 (\$4.00 for microfiche) plus a \$3.00 handling fee, all orders must be prepaid; G.B. Zimmerman, R.M. More, *J. Quant. Spectrosc. Radiat. Transfer* **23**, 517 (1980); R. M. More, *J. Quant. Spectrosc. Radiat. Transfer* **27**, 345 (1982)
13. H. Robey, private communication (2005)
14. S.W. Haan, *Phys. Rev. A* **39**, 5812 (1989)
15. J.D. Moody et al., *J. Phys. IV France* **133**, 863 (2006)
16. J. Edwards et al., *Phys. Plasma* **12**, 056318 (2005)